

## *Ab initio* calculation of optical-mode frequencies in compressed solid hydrogen

Kazutaka Nagao,\* Tomoki Takezawa, and Hitose Nagara

*Division of Materials Physics, Graduate School of Engineering Science, Osaka University, Toyonaka, Osaka 560-8531, Japan*

(Received 1 September 1998)

Vibrational optical-mode frequencies have been calculated for some of the structures recently proposed by theoretical and experimental studies of compressed solid hydrogen, by means of first principles band theoretical treatments using the plane wave basis set, in the local density approximation (LDA) and the generalized gradient approximation (GGA) for the exchange-correlation energy. The results of the GGA are compared with those of the LDA, and both results are compared with recent Raman scattering and infrared absorption experiments. The possible structures of the compressed molecular solid hydrogen at megabar pressures have been discussed in light of vibrational optical modes and their frequencies. The total energy is also calculated in the GGA for some of the candidate structures in the molecular phase as well as those in the atomic phase. The molecular phase persists over 400 GPa, which can result in the metallization prior to the molecular dissociation. The effects of the band gap closure on the frequencies are studied together with the effects of the GGA. The GGA decreases the bond length and hence increases the vibron frequencies, by which the calculated frequencies show excellent agreement with the experiments for the  $Cmc2_1$  structure, while the phonon frequencies are less affected by the GGA. The shorter bond length leads to wider band gaps. The GGA favors the molecular phase more than the atomic phase. Our results of the frequencies suggest that the  $Pca2_1$  structure is most probable in phase II if the molecules are oriented there and the  $Cmc2_1$  is in phase III at pressures under  $\sim 200$  GPa. [S0163-1829(99)07721-8]

### I. INTRODUCTION

Since Wigner and Huntington predicted the pressure induced molecular dissociation of solid hydrogen and its resulting metallic state,<sup>1</sup> such as alkaline metals, more than sixty years have passed. In the meantime high pressure techniques in the laboratories have advanced so much and the substance of celestial interests has changed into a target of experimental challenge in the laboratories.<sup>2,3</sup> The possibility of high-temperature superconductivity has added interest to this substance.<sup>4,5</sup> The possibility of metallization by the band overlapping in the molecular phase before the molecular dissociation has also been predicted and studied intensively by shock compression<sup>3</sup> as well as static compression using diamond anvil cells.<sup>6</sup>

A recent shock-compression experiment<sup>3</sup> reported decrease in the resistivity of liquid deuterium and hydrogen, by about four orders of magnitude, around 140 GPa (100 GPa = 1 Mbar) at the relatively low temperature of a few thousand degrees. A similar experiment also reported the significant deviation of the compressibility of liquid deuterium from that of the former theoretical prediction, which suggests the increased molecular dissociation at elevated temperatures.<sup>7</sup>

Although no evidence of metallization nor molecular dissociation has been confirmed so far by the static compression experiments at room and lower temperatures up to  $\sim 250$  GPa,<sup>8,9</sup> new important experimental data have been obtained and accumulated.<sup>2,8-16</sup> The phase boundaries among three phases in the solid hydrogen and deuterium have been established experimentally,<sup>2,12</sup> and the lattice of the molecular centers has been determined at room temperature to be hcp up to  $\sim 120$  GPa by x-ray experiment.<sup>10</sup> A recent Raman experiment<sup>15</sup> has reported the possibility of further rich phase diagram in ortho-para mixed crystals.<sup>17</sup>

In addition to experimental studies, a large number of theoretical studies have appeared and predicted the molecular dissociation or the metallization in compressed hydrogen. The predicted pressures, however, are widely scattered: the pressure of the metallization ranges over the region of 1–3 Mbar and that of the dissociation over 3–6 Mbar.<sup>18-22</sup> One of the main reasons for the difficulty in the prediction may be the quantum effects<sup>23-26</sup> expected in this lightest element and another reason is the lack of the information of the structures at megabar pressures. The crystal structures in both molecular and atomic phases are essential to the prediction of the pressure of possible metallization by the band overlapping in the molecular phase or the molecular dissociation and its resulting metallization at low temperatures.

Raman and infrared (IR) experiments for the vibrons (intramolecular stretching modes), midlying phonons<sup>8</sup> (translational modes of the molecular centers), and other low-lying phonon and librions<sup>13,16</sup> (the motions of the molecular orientation) at megabar pressures provide important information on the structure and the molecular orientations in the molecular phase of compressed hydrogen. However, theoretical studies of the vibrational modes are rather scarce in the molecular phase except for the vibrons. Some studies treated the vibron frequencies based on the *ab initio* calculations,<sup>24,27,28</sup> and others treated those based on the effective force constants or the effective pair interactions corrected by *ab initio* calculations.<sup>12,29</sup>

Cui, Chen, and Silvera<sup>12</sup> have made a group theoretical analysis of IR and Raman active vibron and phonon modes for several structures proposed at megabar pressures. Recently we have made an *ab initio* calculation of the vibrational frequencies for the hcp structures in the molecular phase.<sup>30</sup> Further extensive theoretical studies on the vibrational modes and their frequencies are needed to analyze the

spectra and to determine the structures and molecular orientations at megabar pressures.

In this paper, we present *ab initio* calculations of the vibrational frequencies based on the local density approximation (LDA) and the generalized gradient approximation (GGA) for the exchange correlation energy. In Sec. II we present the methods and in Sec. III the results of the LDA calculations for the candidate structures at megabar pressures. In Sec. IV the effects of the band gap closure and the effects of the GGA are studied. In Sec. V, after we calculate the total energies in the GGA for some structures of interest, we discuss the possible structures, in light of the optical mode frequencies with concluding remarks in Sec. VI.

## II. METHODS OF CALCULATIONS

In the calculation of the force matrix, we use the frozen-phonon method and the Hellman-Feynman theorem<sup>31</sup> and use the bare Coulomb form of the atomic potential and the exchange-correlation potential of the form of Barth and Hedin<sup>32</sup> in the band theoretical calculations. In this paper we study frequencies at the  $\Gamma$  point in the Brillouin zone (BZ) in the harmonic approximation. The vibrational frequencies at other wave vectors can be obtained through calculations similar to those of the  $\Gamma$  point by the use of supercells which contain several primitive cells in accordance with the period defined by the wave vector.

In the treatment of lattice dynamics, the frequencies at the  $\Gamma$  point can be calculated, in principle, from the dynamical matrix obtained from the forces corresponding to any set of linearly independent displacements of the atoms in the unit cell. However, in the molecular crystals, especially in solid hydrogen, characters of the modes differ from one another somewhat: the frequencies of vibronic modes are much higher than those corresponding to phononlike and librational modes and some librational modes may be lower than the others. Further, in quantum or anharmonic crystals, some low-lying modes may become unstable in the harmonic approximation, which may be stabilized by the higher order terms when they are included by more sophisticated methods, for example, the self-consistent phonon treatment.<sup>33</sup> With these large differences of the frequencies in the molecular crystals, it may be possible to treat the high-lying modes separately from the low-lying modes. This treatment leads to an easier analysis of the modes.

We first analyze the displacements using group theory and obtain the symmetry coordinates corresponding to the irreducible representation for the space group.<sup>34</sup> Using the symmetry coordinates, we can transform, in advance, the entire force matrix into the reduced form which consists of submatrices on the diagonal. The matrix elements of the submatrices are obtained by the use of the displacements corresponding to the symmetry coordinates which belong to the same irreducible representation. By this treatment, we can calculate the frequencies of the modes belonging to an irreducible representation independently from other modes which belong to other irreducible representations. As will be shown below, this treatment can reduce the computational efforts to obtain frequencies corresponding to the modes of interest. They can also enhance the accuracy in the calculation of the matrix elements.

In the construction of the symmetry coordinates, which are obtained from the symmetry vectors calculated by the use of projection operators,<sup>34</sup> we use the ambiguity of the definition of the symmetry coordinates and obtain tentatively those which correspond to the vibronic motion, the librational motion, the phononlike motion, and the uniform translation, so that we can specify the characteristics of the modes. There remains the coupling among the tentative motions when some of the motions belong to the same representation, for which the diagonalization of the submatrix is needed to obtain the normal modes. The symmetry coordinates used in the calculation for the  $Cmc2_1$  structure were given in Ref. 30. For some other candidate structures we obtained the symmetry coordinates using similar procedures as those used for the  $Cmc2_1$ .

To obtain the force matrix we first write the symmetry coordinate as  $q^{ia} = \sum_{n\alpha} C_{ia,n\alpha} r_{n\alpha}$ , where  $i$  labels the representation and  $a$  distinguishes the independent symmetry coordinates belonging to the same irreducible representation and  $r_{n\alpha}$  denotes the Cartesian component  $\alpha$  of the displacement vector of the atom  $n$  in the unit cell. Then we calculate the force  $f_{n\alpha}^{ia}$  which means the Cartesian component  $\alpha$  of the force acting on the atom  $n$  when the displacement corresponding to the symmetry coordinate  $q^{ia}$  is generated in the lattice. From the increments of the above quantities we can obtain the force submatrix

$$\begin{aligned} \Phi_{aa'}^i &\equiv \frac{\partial^2 E}{\partial q^{ia} \partial q^{ia'}} = \sum_{n\alpha} C_{ia,n\alpha} \frac{\partial^2 E}{\partial r_{n\alpha} \partial q^{ia'}} \\ &\equiv - \sum_{n\alpha} C_{ia,n\alpha} (\Delta f_{n\alpha}^{ia'} / \Delta q^{ia'}), \end{aligned} \quad (1)$$

where  $E$  is the total energy per unit cell. We note that

$$\sum_{n\alpha} C_{ia,n\alpha} C_{i'a',n\alpha} = \delta_{ia,i'a'}, \quad (2)$$

and

$$\sum_{i\alpha} C_{ia,n\alpha} C_{ia,n'\alpha'} = \delta_{n\alpha,n'\alpha'}, \quad (3)$$

as can be shown, for example, from the definition of the symmetry coordinates in Table I of Ref. 30. The normal coordinates and the frequencies of the vibrational modes are obtained through the diagonalization of the submatrices whose dimensions are much smaller than that of the total force matrix. The matrix elements corresponding to the uniform translations are trivial and the dimensions of the submatrices containing the uniform translation can be reduced further.

### A. Computation

We set the energy cutoff  $E_{\text{cut}}$  of the plane-wave basis at  $\sim 65$  Ry in our band theoretical calculations at density  $r_s = 1.5$  ( $P \sim 120$  GPa), for which the number of the plane wave is around  $125 \times N$  ( $N$  is the number of atoms in a unit cell). Here the density parameter  $r_s$  is the radius of a sphere whose volume is equal to the volume per electron in units of Bohr radius  $a_0$ . We fixed the number of the plane waves for

all densities, so the energy cutoff  $E_{\text{cut}}$  changes at each density:  $E_{\text{cut}} \sim 60$  Ry at the lowest density we studied,  $r_s = 1.6$  ( $P \sim 70$  GPa), and  $E_{\text{cut}} \sim 75$  Ry at  $r_s = 1.4$  ( $P \sim 200$  GPa). These values of the energy cutoff are proved to be sufficient by checking the results with increased energy cutoff of 80 Ry at  $r_s = 1.6$ .

For sufficiently converged wave functions in the band calculation, we set the number of iteration for the self-consistency at 6–8 which is about 2 or 3 times as many as the number needed in the total energy calculations, because the errors in the total energy are of second order in the errors of the wave functions, as is guaranteed by the variational principle for the total energy, while those in the forces are of first order. We sampled about  $2000/N$   $\mathbf{k}$  points in the BZ, which is proved to be sufficient in the present studies. We checked the forces by comparing the Hellman-Feynman forces with the derivatives of the total energy with respect to the displacements.

We optimized the bond length through total energy minimization in each structure and at each density. In the total energy, we included energy correction which comes from the plane waves with energy larger than the energy cutoff. The energy correction, for which we used a perturbational treatment,<sup>35</sup> gives a slightly shorter bond length.

In the evaluation of the force matrix, we set the amplitude of the symmetry coordinate within the harmonic region. We show in Fig. 1 the forces as functions of the symmetry coordinates for the vibronic modes. We note that the harmonic regions of the forces are wider for the out-of-phase vibronic, librational, and phononlike modes than for the in-phase vibronic mode, by about five times. The amplitudes we used in our calculation give the displacement of each atom around  $0.001 a_0$  for the vibronic motion and around  $0.005 a_0$  for the phonon and librational motions. We have checked the remaining anharmonicity by inverting the sign of all displacements and recalculating the forces and the frequencies for the modes whose force have even order terms in the displacements, or by changing the amplitudes of the displacements for the mode not having even order terms, depending upon the symmetry property of the modes.<sup>30</sup>

### B. The GGA for the exchange correlation energy

Underestimation of the band gap is one of the well-known shortcomings in the electronic-structure calculation using the LDA. The GGA for the exchange correlation energy has been proposed to improve some shortcomings of the LDA results.<sup>36</sup>

The effects of the GGA are not all clear when it is used in the calculation for the simple diatomic molecules at high pressure. It has, however, been reported that the GGA improves the bond length of the isolated hydrogen molecule, although the GGA does not necessarily improve the bond length for other diatomic molecules.<sup>37</sup> The bond length of the hydrogen molecule is an important quantity in the calculation of the vibrational frequencies, especially for the frequencies of the vibronic modes.

The band gaps are also sensitive to the bond length, which changes the pressure at which band gap closes. For example, in the  $Cmc2_1$  structure which will be studied below, the optimum bond length at  $r_s = 1.45$  is  $1.427 a_0$ , at which the

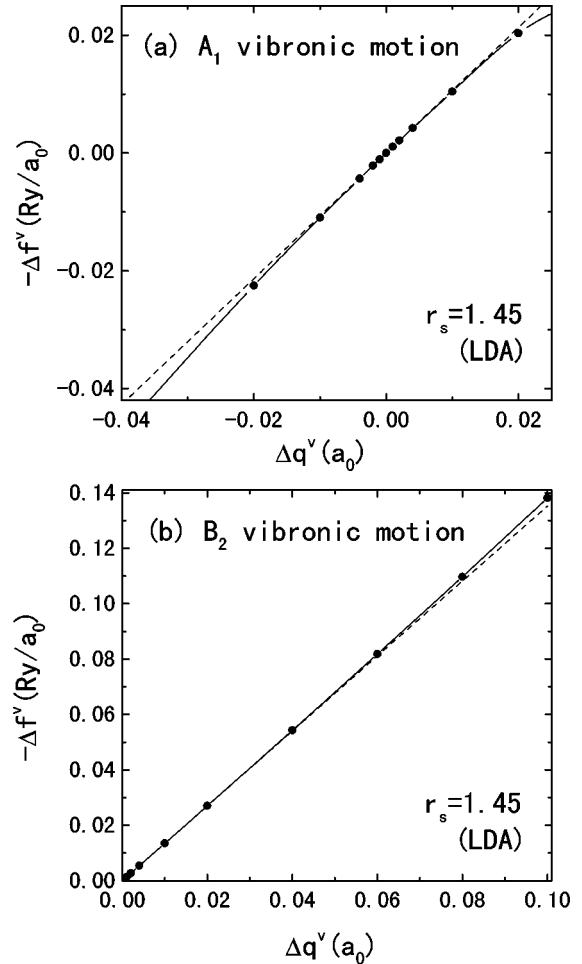


FIG. 1. Harmonic regions of the forces for vibronic motions in the  $Cmc2_1$  structure. The force  $f^v = -\partial E / \partial q^v$  is plotted as a function of the vibron symmetry coordinate  $q^v$  where  $E$  is the energy per unit cell. The broken lines are the tangents. The force of the  $B_2$  vibronic motion is odd with respect to the sign change of the displacement. The linear region of the force for the  $A_1$  vibronic motion (in-phase motion) is much narrower than that for the  $B_2$  vibronic motion (out-of-phase motion). In the present study, we used an amplitude  $q^v$  of  $0.002 a_0$  for both vibronic motions.

LDA band gap (indirect gap) is closed. When the bond length is set at  $1.38 a_0$  in the same structure, the LDA band gap increases to  $0.45$  Ry. The decrease of the bond length by the GGA and the resulting change of the bands may change the forces, for which we need more studies of the effects of the GGA.

Recently, simplified versions of the GGA have been proposed, and in our calculations we used the simplified version of the GGA given by Perdew *et al.*<sup>38</sup> for our spin-unpolarized case. We first study the vibrational frequencies in the LDA in the next section and in the subsequent section we study the effects of the GGA on the band gaps and the frequencies together with the effect of the band gap closure.

### III. LDA RESULTS FOR SOME OF CANDIDATE STRUCTURES

Although the nature of the three phases in the compressed molecular hydrogen<sup>2,12</sup> are not all clear, the following specu-

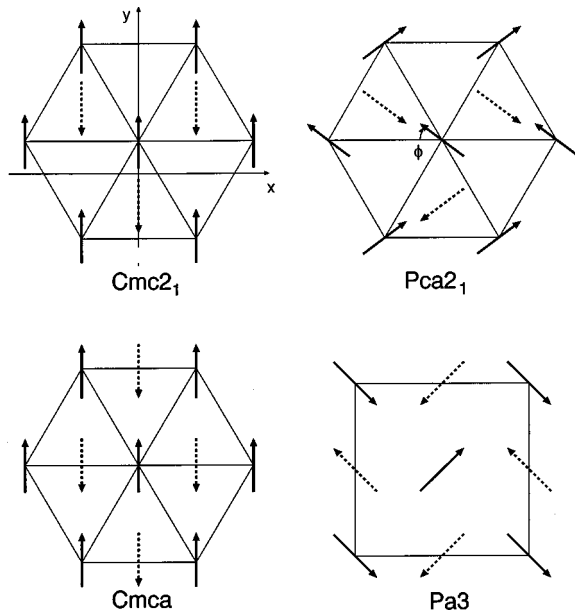


FIG. 2. Illustration of the structures. Arrows indicate the direction of molecular axes whose direction cosines with the  $z$  axis are positive. The  $Cmc2_1$  structure is obtained by setting the azimuthal angle  $\phi=90^\circ$  in the  $Pca2_1$  structure. The  $Pca2_1$  structure contains four molecules, i.e., eight atoms in the primitive cell. The  $Cmca$  structure is obtained by displacing one molecule along the  $y$  direction in the  $Cmc2_1$  structure. By setting the polar angle  $\theta=0^\circ$  in the  $Pca2_1$  or the  $Cmc2_1$  structure the  $m$ -hcp( $P6_3/mmc$ ) structure is obtained. For the  $Cmc2_1$ , the  $x$  and  $y$  axes are shown.

lative guess exists at low temperatures.

In phase I (low pressure phase), molecules form a hcp lattice and are in a quantum rotating state. In the region of higher pressure, i.e., in phase II (broken symmetry phase), molecules are thought to be probably in states of some partial orientational order.<sup>13</sup> At pressures higher than around 150 GPa, i.e., in phase III (hydrogen A phase) molecules are considered to be in states of possible orientational order.

The recent IR and Raman experiments have observed some of the vibronic modes<sup>2,11</sup> in hydrogen and deuterium in the three phases along with an IR active mode lying in  $1600\text{--}1900\text{ cm}^{-1}$  in hydrogen in phase III which is most likely a phonon mode.<sup>8</sup> A very recent experiment has also observed low-lying phonon and librational modes in phases II and III for hydrogen.<sup>13,16</sup>

Some structures have been proposed at high pressures from experimental as well as theoretical studies. Experimental studies<sup>2,10,12,39</sup> proposed the hcp to be the most probable lattice of the molecular centers, and many theoretical studies<sup>18,21,27</sup> supported hcp structures. One of the very recent Raman experiments<sup>16</sup> has proposed a possibility of the  $Pa3$  structure in which molecular centers form the fcc lattice, or the  $Cmca$  structure in which molecular centers deviate from the hcp lattice sites, in phase II. Further, recent LDA calculations have also proposed the possibility of the displacement of the molecular centers from the hcp sites.<sup>33,40</sup>

We study vibrational modes for the structures with those lattices of the molecular centers assuming some patterns of the molecular orientation. In Fig. 2 we illustrate the structures we study in this paper. Characteristics of the symmetry coordinates in those structures are listed in Table I.

## A. The hcp structures

We study the hcp lattice of the molecular centers intensively, changing the molecular orientation. We take the  $Cmc2_1$  and the  $m$ -hcp structures as the structure containing two molecules in the primitive cell, and study the  $Pca2_1$  structure which contains four molecules in the primitive cell.

### 1. The $Cmc2_1$ structure

This structure was first studied by Kaxiras, Broughton, and Hemley<sup>41</sup> in their total energy calculations. In the  $Cmc2_1$  structure the indirect band gap in the LDA closes around  $r_s\sim 1.45$  ( $P\sim 150$  GPa). We show the pressure dependences of the vibrational frequencies in Fig. 3. The pressure dependences of the frequencies of the vibronic modes are in good agreement with the experiments, although the frequencies themselves are somewhat lower than the experimental values.<sup>30</sup> The frequency of the mid-lying phonon mode is also in good agreement with the experiments.

For this structure we tried the following two types of calculations in the treatment of the Fermi surface to check the results at densities where the band gaps are closed. The first type is to use the same occupation of one-electron states before and after generating the displacements of the atoms, which corresponds to ignoring the effects of the changes of the Fermi surface. This type of calculation is used for the calculation of the forces throughout this paper. The second is to use the tetrahedron method for the  $k$ -point sampling in the calculation of the forces. The results are shown in Fig. 4 at  $r_s=1.45$  ( $P\sim 150$  GPa) and  $r_s=1.40$  ( $P\sim 200$  GPa). At  $r_s=1.40$ , where the indirect band gap in the LDA is closed with considerable overlapping, the in-phase vibron frequency by the second type calculation is lower by about  $200\text{ cm}^{-1}$  than that of the first type, as is shown in Fig. 4. At  $r_s=1.45$  where the band overlapping is small in the LDA, the first and the second types of the calculation gave nearly same values for both vibron frequencies. The frequencies of phononlike modes, however, remains at nearly same values by both types of the calculation at both densities. When the band gaps are open, the two methods are identical.

We also checked the effects of the decrease of  $c/a$  which is observed in the experiments at low densities and at room temperature. The effects on the frequencies of the vibronic and the phononlike modes are rather small for  $c/a=1.58$  (extrapolated value from the data in Ref. 10) at  $r_s=1.45$  ( $P\sim 150$  GPa), as is shown in Fig. 4.

We study then the normal modes in the  $Cmc2_1$  structure. In this structure, the vibronic, librational, and phononlike motions belong to the same representation as are shown in Table I. At high densities the couplings among the motions are expected to become strong. However, our results show that the couplings between the vibronic motions and the phonon or the librational motions are weak and their mixing are small up to about  $\sim 200$  GPa, owing to the large difference in the diagonal elements of the force matrix, although those will increase at further higher densities. The mixing of the librational motions with the phonon ones is large, as is observed from the normal coordinates given in Table II in which we show the mixing among the motions.

Finally we note that some modes with  $\mathbf{k}\neq\mathbf{0}$  in the  $Cmc2_1$  structure are unstable in the harmonic approximation. For

TABLE I. Characteristics of the symmetry coordinates used in our calculations of the vibrational frequencies at the  $\Gamma$  point in the Brillouin zone for the  $Pca2_1$ ,  $Cmc2_1$ ,  $Cmca$ ,  $m$ -hcp, and  $Pa3$  structures. Each symmetry coordinate is designated by the name of the irreducible representation followed by its characteristics in the parentheses. The letters  $v$ ,  $p$ ,  $l$ , and  $t$  are the characteristics and denote the vibronic, phonon, and librational motions, and the uniform translation, respectively. The  $\theta$  or  $\phi$  in the parentheses denotes the angle which changes its value by the motion, and  $x$ ,  $y$ , or  $z$  the direction of the motion, and  $xz$  or  $yz$  the plane in which molecules move. The vibronic motions in the first row are of in-phase and other vibronic motions are of out-of-phase. The letters R and I in the brackets indicate the Raman and IR activities, respectively. Each symmetry coordinate in the same row transfers to that of other structure when one structure is transformed into the other by changing the orientation of the molecules or by displacing the molecular centers, except for those of the  $Pa3$ .

$Pca2_1$		$Cmc2_1$		$Cmca$		$m$ -hcp <sup>a</sup>		$Pa3^b$			
$A_1(v)$	[R,I]	$A_1(v)$	[R,I]	$A_g(v)$	[R]	$A_{1g}(v)$	[R]	$A_g(v)$	[R]		
$A_1(l-\theta)$	[R,I]	$A_1(l-\theta)$	[R,I]	$A_g(l-\theta)$	[R]	$E_{2u}(l-yz)$	[R]				
$A_1(l-\phi)$	[R,I]							$E_g(l)$	[R]		
$A_1(p-x)$	[R,I]							$E_g(l)$	[R]		
$A_1(p-y)$	[R,I]	$A_1(p-y)$	[R,I]	$B_{1u}(p-y)$	[I]	$E_{2g}(p-y)$	[R]				
$A_1(t-z)$		$A_1(t-z)$		$B_{1u}(t-z)$		$A_{2u}(t-z)$		$T_g(v)$	[R]		
								$T_g(v)$	[R]		
$A_2(v)$	[R]							$T_g(v)$	[R]		
$A_2(l-\theta)$	[R]										
$A_2(l-\phi)$	[R]	$A_2(l-\phi)$	[R]	$B_{1g}(l-\phi)$	[R]	$E_{2u}(l-xz)$	[R]	$T_g^{(1)}(l)$	[R]	$T_g^{(2)}(l)$	[R]
$A_2(p-x)$	[R]	$A_2(p-x)$	[R]	$A_u(p-x)$		$E_{2g}(p-x)$	[R]	$T_g^{(1)}(l)$	[R]	$T_g^{(2)}(l)$	[R]
$A_2(p-y)$	[R]							$T_g^{(1)}(l)$	[R]	$T_g^{(2)}(l)$	[R]
$A_2(p-z)$	[R]										
								$A_u(p)$			
$B_1(v)$	[R,I]										
$B_1(l-\theta)$	[R,I]							$E_u(p)$			
$B_1(l-\phi)$	[R,I]	$B_1(l-\phi)$	[R,I]	$B_{2g}(l-\phi)$	[R]	$E_{1g}(l-xz)$		$E_u(p)$			
$B_1(p-y)$	[R,I]										
$B_1(p-z)$	[R,I]							$T_u(t-x)$			
$B_1(t-x)$		$B_1(t-x)$		$B_{3u}(t-x)$		$E_{1u}(t-x)$		$T_u(t-y)$			
								$T_u(t-z)$			
$B_2(v)$	[R,I]	$B_2(v)$	[R,I]	$B_{3g}(v)$	[R]	$B_{1u}(v)$					
$B_2(l-\theta)$	[R,I]	$B_2(l-\theta)$	[R,I]	$B_{3g}(l-\theta)$	[R]	$E_{1g}(l-yz)$		$T_u^{(1)}(p-x)$	[I]	$T_u^{(2)}(p-x)$	[I]
$B_2(l-\phi)$	[R,I]							$T_u^{(1)}(p-y)$	[I]	$T_u^{(2)}(p-y)$	[I]
$B_2(p-x)$	[R,I]							$T_u^{(1)}(p-z)$	[I]	$T_u^{(2)}(p-z)$	[I]
$B_2(p-z)$	[R,I]	$B_2(p-z)$	[R,I]	$B_{2u}(p-z)$	[I]	$B_{2g}(p-z)$					
$B_2(t-y)$		$B_2(t-y)$		$B_{2u}(t-y)$		$E_{1u}(t-y)$					

<sup>a</sup>For the  $m$ -hcp, doubly degenerate modes designated by  $E_{1g}$ ,  $E_{2g}$ ,  $E_{1u}$ , and  $E_{2u}$  have two independent symmetry coordinates, respectively.

<sup>b</sup>For the  $Pa3$ , two triply degenerate librational modes belonging to the  $T_g$  representation are distinguished by the superscript (1) and (2), which is the same for the phonon modes belonging to the  $T_u$  representation. Each triply degenerate mode has three independent symmetry coordinates.

example, the mode at a zone boundary point becomes unstable, for which Mazin and Cohen<sup>42</sup> studied the potential profile. They showed the highly anharmonic potential for this mode and the possible large fluctuations over the low potential barrier although the fluctuation studied by them is a coherent motion and needs to be studied more.<sup>33,43-45</sup> If such large fluctuations of azimuthal librational motion occur, the average structure can be the  $Cmc2_1$ .

## 2. The $Pca2_1$ structure

This structure is known as the structure which has the lowest energy in the hcp lattices when the intermolecular interaction is assumed to be electric quadrupole-quadrupole (EQQ) one.<sup>46</sup> In this structure, molecules keep away with each other orientationally from the neighboring molecules to a higher degree than the  $Cmc2_1$ , and hence the band gap in the LDA persists to  $\sim 190$  GPa. We optimized the bond

length in the  $Pca2_1$  but fixed the polar and azimuthal angles ( $\theta, \phi$ ) at ( $55^\circ, 43.5^\circ$ ), and calculated the frequencies. The optimum bond length decreases with increasing pressure, which is shown in Table III.

The calculated vibron frequencies in the LDA do not soften as much as the experiments show in phase III with increasing pressure, which is shown in Fig. 3. The frequency of the phononlike mode is close to the experiments.

## 3. The $m$ -hcp structure

We study then the  $m$ -hcp structure<sup>18</sup> by setting the polar angle  $\theta=0^\circ$ , using the same symmetry coordinates as those for the  $Cmc2_1$ . In this structure, the LDA band gap closes at considerably low density  $r_s$  larger than  $\sim 1.60$ . For this structure, we made the same calculations as those for the  $Cmc2_1$ . A remarkable point in this structure is that the vibron frequencies are considerably lower than those of other

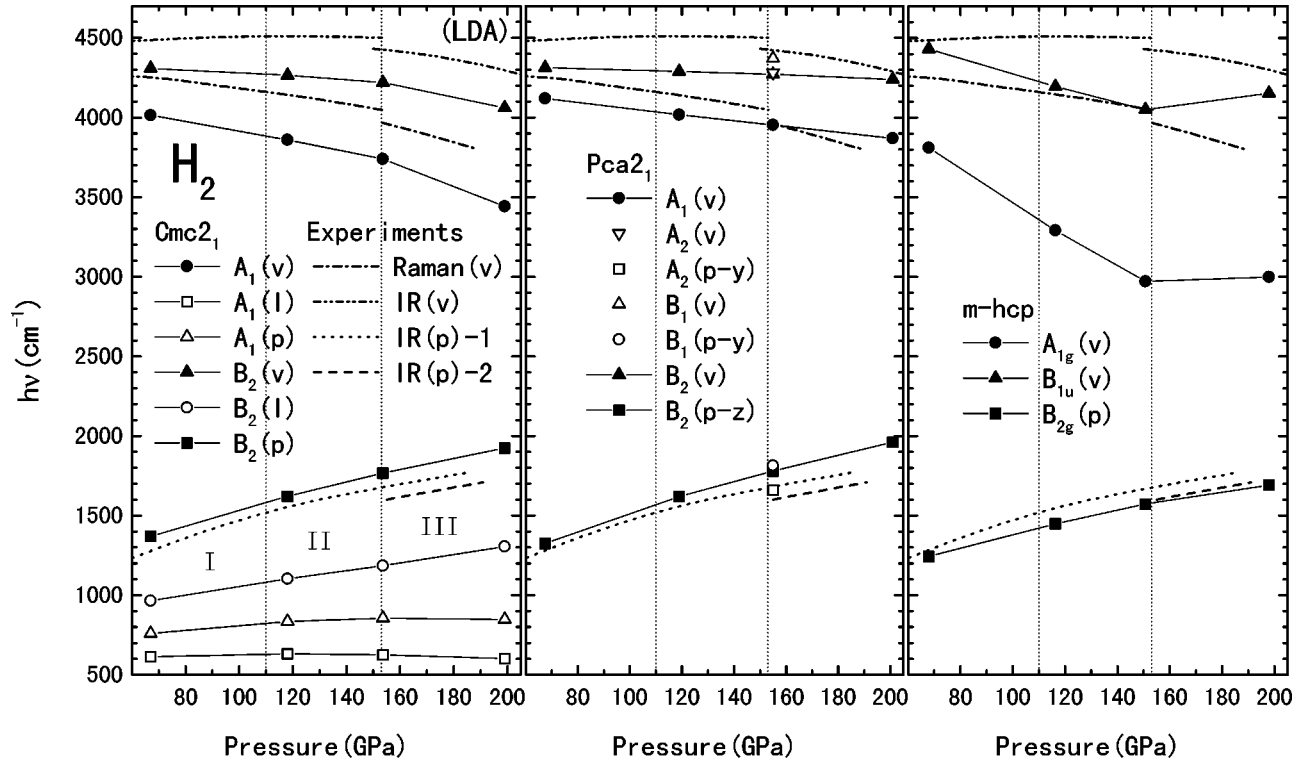


FIG. 3. Pressure dependences of the frequencies of vibrational modes in the LDA for the structures with hcp lattice of the molecular centers. The marks show our data points and lines connecting those points are guides to the eye. The ( $v$ ), ( $l$ ), and ( $p$ ) denote the vibronic, librational, and phononlike modes, respectively. Experimental data are taken from Ref. 8 ( $p$ -H<sub>2</sub>) for IR( $p$ )-2 and from Refs. 2 and 53 ( $o$ - $p$  mixed H<sub>2</sub>) for the others. The vertical broken lines show the boundaries of the phases I, II, and III for hydrogen taken from Refs. 2 and 54.

structures with hcp lattice studied here although the frequencies of the phononlike modes are close to those of the other structures, as is shown in Fig. 3.

### B. Layered structures

Recent theoretical studies reported that structures in which the molecular centers deviate from the hcp lattice sites have lower energies than those of the hcp. Edwards *et al.*<sup>33</sup> studied the  $Cmca$  structure and showed that the energy of the  $Cmca$  structure becomes lower than that of the  $Cmc2_1$  with molecules sitting at the hcp lattice site at  $\sim$  ninefold compression.

We observe that the  $Pca2_1$  structure changes into the  $Cmc2_1$  structure at the special value of the azimuthal angle  $\phi=90^\circ$  as shown in Fig. 2. Also the  $Cmc2_1$  structure permits the displacement of one of the two molecules in the unit cell in a direction. The  $Cmc2_1$  transforms into the  $Cmca$  at some value of the displacement, which can be seen in Fig. 2.

We study the  $Cmc2_1$  structure by displacing the molecule on the line from the hcp site to the  $Cmca$  site. In Fig. 5 we show the total energy and some of the vibrational frequencies, as a function of the displacement. The energy minimum in the LDA lies near the  $Cmca$ . In the  $Cmca$  structure band gaps close at considerably low density,  $r_s$  larger than  $\sim 1.60$ , for the optimum bond length.

We calculated the frequency of the  $Cmca$  at the optimum bond length for fixed polar angle of  $60^\circ$  at each density, which is shown in Fig. 6. The calculated vibron frequencies are much lower than the experimental values, as is expected from the closed band gaps. The frequency of the midlying

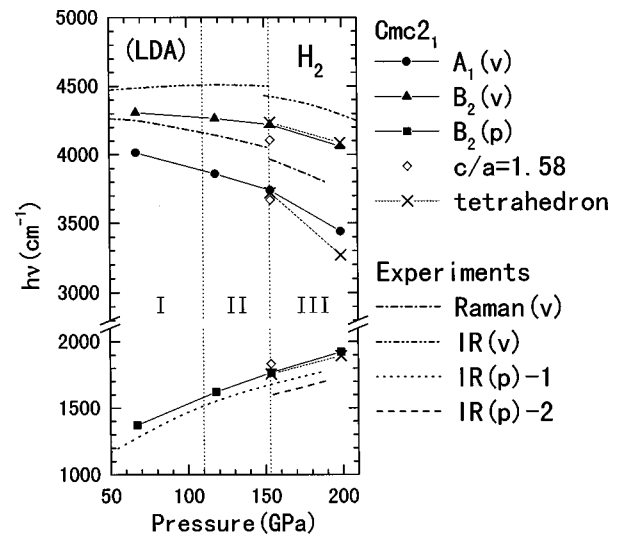


FIG. 4. Checking the results of the calculation for the  $Cmc2_1$  structure. The frequencies connected by the solid lines are calculated by the method of using the same occupation of one-electron states before and after generating the displacements of the atoms. (See the text in Sec. III A 1.) The results are checked by the tetrahedron methods of the  $\mathbf{k}$ -point sampling in the calculation of the forces at  $r_s=1.40$  ( $P\sim 200$  GPa) and  $r_s=1.45$  ( $P\sim 150$  GPa). The effects of change of the  $c/a$  value of the hcp are also examined at  $r_s=1.45$  ( $P\sim 150$  GPa) with data points in the same figure.

TABLE II. Mixing among the vibronic, phonon, and librational motions in the  $Cmc2_1$  structure. The normal coordinates  $\tilde{q}^{ia}$  are decomposed into the symmetry coordinates,  $q^{ia}$  used in our calculations, as  $\tilde{q}^{ia} = \sum_a c_{ia} q^{ia}$ , with  $\sum_a c_{ia}^2 = 1$ . The amplitude,  $c_{ia}$ , is obtained by diagonalizing the dynamical matrix. Here the notations  $c_v$ ,  $c_l$ , and  $c_p$  are used for this structure in place of the  $c_{ia}$  to show the motions explicitly, where  $v$ ,  $l$ , and  $p$  denote the vibronic, librational, and phonon, respectively. The calculations are done in the LDA.

$r_s$	Frequency $h\nu(\text{cm}^{-1})$	$c_v$	$c_l$	$c_p$
$A_1$ modes				
1.40	601	0.05570	0.71855	0.69324
	847	0.02116	-0.69501	0.71869
	3441	0.99822	-0.02536	-0.05392
1.50	632	0.01628	0.91291	0.40783
	835	0.02075	-0.40811	0.91270
	3860	0.99965	-0.00640	-0.02559
$B_2$ modes				
1.40	1305	0.07206	0.99706	-0.02606
	1924	0.00120	0.02604	0.99966
	4060	0.99740	-0.07207	0.00068
1.50	1102	0.04279	0.99854	-0.03294
	1621	0.00083	-0.03300	-0.99946
	4265	0.99908	-0.04274	0.00224

phononlike mode in this structure, where the molecular centers are displaced considerably from the hcp sites, is a little higher than those of the hcp structures. These results of the frequencies exclude the possibility of the  $Cmca$  in phase II and in phase III at pressures lower than  $\sim 200$  GPa.

### C. The fcc structures

In the very recent Raman experiment on pure parahydrogen at megabar pressures, Goncharov *et al.*<sup>16</sup> proposed the possibility of the  $Pa3$  structure in phase II from the observation that the Raman phonon line disappears there. In this structure too, molecular orientations are such that they keep away with each other from the neighboring molecules to a high degree, similar to the  $Pca2_1$  of the hcp lattice, and the band gap persists to over  $\sim 200$  GPa.

TABLE III. Comparison of the optimum bond lengths,  $R_b$ , in the LDA with those in the GGA. For the  $Cmc2_1$ , the optimum molecular orientation  $\theta$  is also shown. The molecular orientation is fixed at  $(\theta, \phi) = (55^\circ, 43.5^\circ)$  in the  $Pca2_1$  and at  $\theta = 60^\circ$  in the  $Cmca$ . The bond length  $R_b$  is in units of Bohr radius  $a_0$  and the polar angle  $\theta$  is in degrees. The asterisk on the figures of  $R_b$  show that the band gap is closed at that value.

$r_s$	LDA						GGA			
	$Cmc2_1$		$Pca2_1$	$Cmca$	$m$ -hcp	$Pa3$	$Cmc2_1$		$Pca2_1$	$Cmca$
	$R_b$	$\theta$	$R_b$	$R_b$	$R_b$	$R_b$	$R_b$	$\theta$	$R_b$	$R_b$
1.40	1.447*	47.3	1.412*	1.542*	1.500*	1.390	1.383*	52.0	1.372	1.480*
1.45	1.427*	48.8	1.415	1.529*	1.510*	1.401	1.382	51.2	1.376	1.467*
1.50	1.427	48.6	1.421	1.517*	1.481*	1.410	1.385	50.2	1.379	1.455*
1.60	1.434	48.0	1.432	1.485*	1.448*	1.426	1.391	49.5	1.387	1.407*

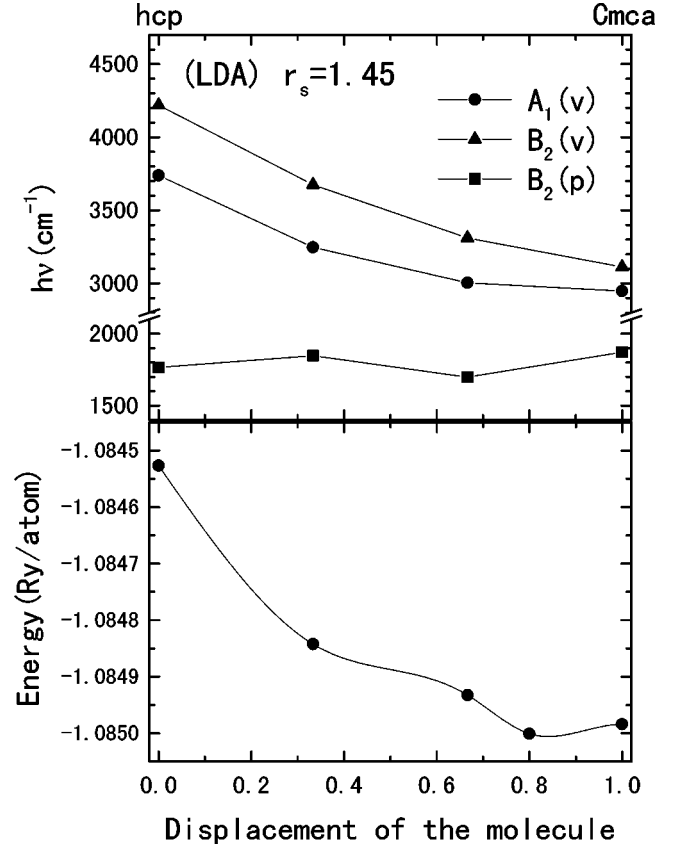


FIG. 5. Total energy and some frequencies in the LDA as functions of the displacement of the molecular center along the  $y$  axis in the  $Cmc2_1$  structure. The bond lengths are optimized but the molecular orientation is fixed at  $\theta = 60^\circ$ , in the calculations. The distance from the center of the triangle in the hexagonal plane to the mid-point of the base line of the triangle is normalized to unity.

There exist four vibronic modes in this structure, and out-of-phase modes are triply degenerate, as is shown in Table I. The pressure dependences of the vibron frequencies calculated in the LDA are somewhat different from the experiments, especially in phase III, which are shown in Fig. 6. The frequency of the midlying phonon mode, however, is very close to the experimental value.

### IV. EFFECTS OF THE BAND GAP CLOSURE AND THOSE OF THE GGA

We study, in this section, the effects of the band gap closure on the bond length and the vibrational frequencies

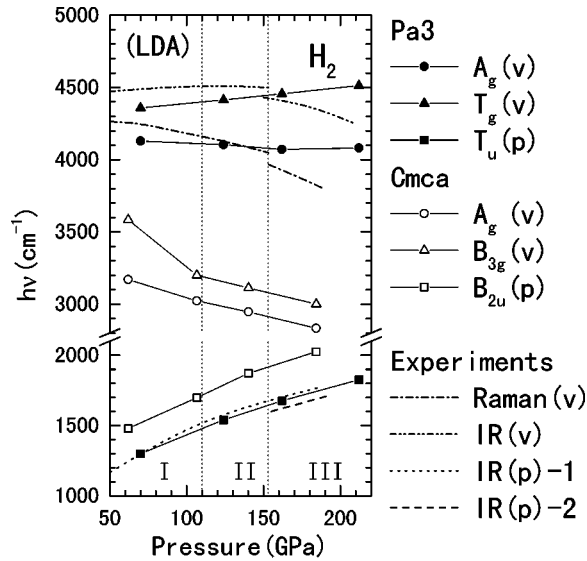


FIG. 6. The LDA results of the pressure dependences of the frequencies for  $Pa3$  and  $Cmca$  structures. In the  $Pa3$  structure molecular centers form the fcc lattice. The meaning of the symbols and letters designating the lines are same as those explained in Fig. 3.

and effects of the GGA on the band gaps and the frequencies, for some of the structures studied above.

#### A. Effects of the band gap closure

The band gaps in the LDA close at considerably low pressures, lower than 60 GPa, in the  $m$ -hcp and  $Cmca$  structures, while in the  $Cmc2_1$  structure with molecules at hcp lattice sites, the gap closes at  $\sim 150$  GPa, and in the  $Pca2_1$  and the  $Pa3$  structure band gaps persist to over 190 GPa, as was studied in the previous section. Those results show that the band gaps persist to higher pressures in such structures as the molecules orient to keep their atoms away from those in the neighboring molecules than in such structures as to keep their atoms close. The GGA gives the similar results. In Fig. 7 we show the GGA electronic band structures of the  $Cmc2_1$  comparing with those of the  $m$ -hcp and the  $Cmca$ , by which we show examples of changes in the band shapes when the molecular orientation is changed or the displacement of the molecular centers occurs.

As was studied in the previous section, the structures with closed band gaps have considerably low vibronic frequencies. The band gap closure seems to affect little on the frequencies of the phononlike modes. We summarize in Table III the optimum bond length in the LDA for some of the structures and compared with those in the GGA. We observe that the bond lengths decrease with increasing pressure in the pressure region of open band gaps and they turn to increase when the band gaps are closed. Those results imply that the band gap closure is related with the bond length and hence strongly related with the frequencies of the vibronic modes, while it is related less with phononlike modes.

There remains a question of whether the band gap closure originating from the shortcoming of the LDA may affect the present results or not. However, as will be shown in the following subsection, in the GGA, the band gaps are open at least to  $\sim 190$  GPa for the  $Cmc2_1$  and the  $Pca2_1$  struc-

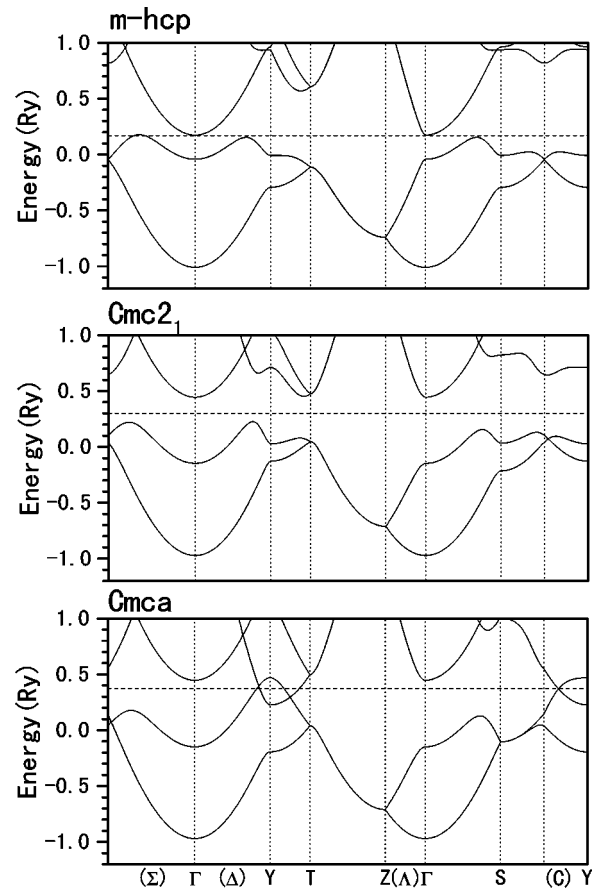


FIG. 7. Changes of the band structures in the GGA among the  $Cmc2_1$ ,  $Cmca$ , and  $m$ -hcp structures at  $r_s = 1.6$ . The base centered orthorhombic unit cell containing two molecules is used for all structures in plotting the band structures with the same axes as that shown for the  $Cmc2_1$  in Fig. 2. The bond length is set at  $1.40 a_0$  for all structures and molecular orientation is set at  $\theta = 60^\circ$  for the  $Cmc2_1$  and  $Cmca$  structures. The  $m$ -hcp structure is obtained from the  $Cmc2_1$  by setting the molecular orientation along the  $c$  axis and the  $Cmca$  by displacing the molecular center (see the text). The LDA results are similar to those shown here but the density corresponding to the same band gap is lower than that of the GGA.

tures, and our results of the frequencies for those structures are free from the problem up to  $\sim 190$  GPa. We note also that the band gaps possibly persist to further higher pressure if the calculations are made beyond the GGA.

#### B. Effects of the GGA

The indirect band gaps are sensitive to the bond length, as was shown in the preceding subsection. The GGA affects the bond lengths, and we study, in this subsection, its effects on the bond length and hence on the band gaps and the vibrational frequencies. The GGA gives shorter bond lengths than the LDA, as is shown in Table III, and the wider band gap is attributed to the shorter bond length by the GGA in addition to the tendency of the wider band gaps inherent to the GGA, as is shown in Table IV. In the GGA, the vibron frequencies shift upward due to the increased bond strength in the molecule. However, the frequency shifts of phononlike modes are small. We recalculate the vibrational frequencies for the  $Cmc2_1$ , the  $Pca2_1$ , and the  $Cmca$  structure in the GGA.

TABLE IV. Band gaps in the  $Cmc2_1$  structure at  $r_s = 1.45$  calculated by the LDA and the GGA, in units of  $eV$ . The molecules sit on the hcp site with the orientation  $\theta = 55^\circ$ .

Point	LDA	GGA
(a) Bond length $1.43 a_0$		
$\Gamma \leftrightarrow \Gamma$	7.028	7.283
$T \leftrightarrow T$	4.048	4.232
indirect <sup>a</sup>	-0.513	0.172
(b) Bond length $1.38 a_0$		
$\Gamma \leftrightarrow \Gamma$	7.433	7.711
$T \leftrightarrow T$	4.609	4.828
indirect <sup>a</sup>	0.447	0.796

<sup>a</sup>The difference between the  $\Gamma$  and the top of the  $\Gamma$ -Y.

### 1. The $Cmc2_1$ structure—in the GGA

In Fig. 8 we show the frequencies by the GGA calculations for this structure. The agreement of the pressure dependences of the frequencies with those of the experiments seems to be excellent for the vibron modes of the hydrogen in phase II.

Here we briefly mention the effects of the anharmonic terms. Generally anharmonic terms give rise to the coupling of the modes obtained in the harmonic approximation at the  $\Gamma$  point with all modes in the Brillouin zone.<sup>47</sup> Kohanoff *et al.*<sup>27</sup> studied the effects on the vibrons phenomenologically by an analysis of the experimental values of the vibron frequencies. The experimental results show that the frequency of the Raman vibron of hydrogen is lower than that of the deuterium multiplied by the factor of  $\sqrt{2}$ , and that the frequency of IR vibron is similar to that of the Raman vibron though the difference is smaller than the Raman vibron,<sup>11,48</sup> as is shown in Fig. 8. The differences of the vibron frequen-

cies between hydrogen and deuterium (multiplied by the  $\sqrt{2}$ ) come from the anharmonicity, if the adiabatic approximation is valid for both hydrogen and deuterium.

It can be thought that our frequencies of harmonic approximation should come over the deuterium values obtained above, because the anharmonicity is larger in the hydrogen than in the deuterium. If we consider the effects of the anharmonic terms, our results are thought to be in good agreement with those of the experiments rather in phase III, which may suggest the possibility of the  $Cmc2_1$  structure in phase III.

### 2. The $Pca2_1$ structure—in the GGA

The vibron frequencies shift upward by the GGA, as is shown in Fig. 8, and the frequencies become higher than the experimental results in phase III. We point out that the calculated frequency of the in-phase vibron mode is very close to those of the experiments for deuterium in phase II, which is similar to the  $Cmc2_1$  in phase III.

The LDA bond length  $1.415 a_0$  at  $r_s = 1.45$  in this structure reduces to  $1.376 a_0$  in the GGA, which are very close to  $1.373 a_0$  (at  $P = 150$  GPa) of Kohanoff *et al.*<sup>27</sup> We note here that our GGA results of vibron frequencies in this structure, however, decrease at pressures higher than  $\sim 100$  GPa, which is in contradiction to the Kohanoff *et al.* raw data of the frequencies<sup>27</sup> showing increase with pressure. We used a bare Coulomb form of the atomic potential in our calculations while they used their pseudopotential. They also used the  $\mathbf{k} \cdot \mathbf{p}$  method in the calculation of the electronic states.<sup>49</sup>

### 3. The $Cmca$ structure—in the GGA

The calculated frequencies are also shown in Fig. 8. The vibron frequencies are considerably lower than the experi-

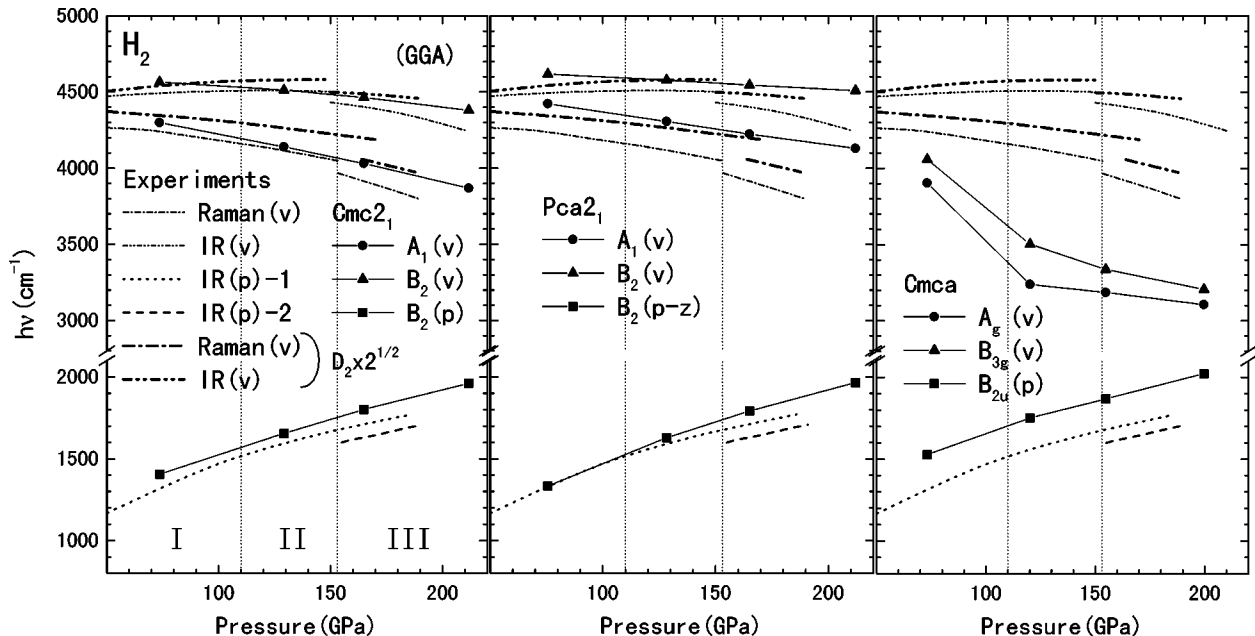


FIG. 8. Pressure dependences of the frequencies recalculated by the GGA for the  $Cmc2_1$ ,  $Pca2_1$ , and  $Cmca$  structures. The meanings of the symbols and letters designating the lines are same as those explained in Fig. 3. In the figures, the experimental values for the vibron frequencies of deuterium (Refs. 11,48) multiplied by the factor  $\sqrt{2}$  are shown. The boundary between the phases I and II for deuterium lies  $\sim 30$  GPa, and that between the phases II and III lies at nearly same pressure. (See, for example, Ref. 12.)

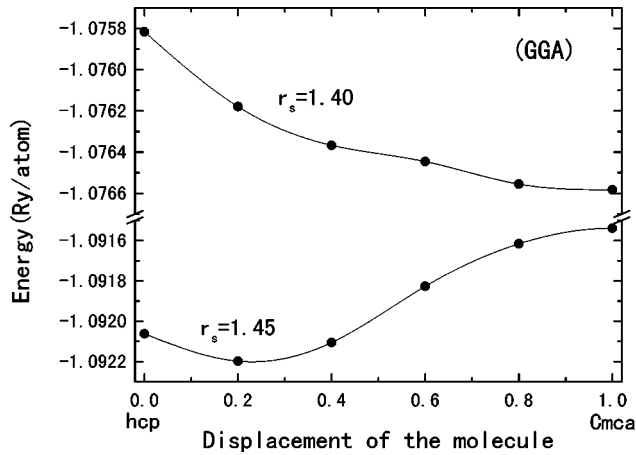


FIG. 9. Total energy in the GGA as a function of the displacement of the molecular center along the  $y$  axis in the  $Cmc2_1$  structure. The structure is optimized in the similar condition as is used in Fig. 5.

ments, even in the GGA. The frequencies of the midlying phonon modes are not affected by the GGA.

As we mentioned in the previous section, the  $Cmc2_1$  permits the displacement of one of the two molecules in the unit cell. The GGA total energy of the  $Cmc2_1$  as a function of the displacement of the molecular center differs somewhat from the LDA one. We show the results in Fig. 9. At  $r_s = 1.45$  the total energy is minimum at the intermediate point on the line from the hcp site to the  $Cmca$  one, while, at  $r_s = 1.40$ , the minimum energy is near the value of the displacement corresponding to the  $Cmca$  structure.<sup>43,44</sup>

## V. STRUCTURES OF SOLID HYDROGEN AT MEGABAR PRESSURES

We studied in Secs. III and IV the vibrational frequencies. Before we discuss the structures of the hydrogen in the molecular phase from the view point of the vibrational frequencies and their Raman and IR activities, we study the total energies in the GGA for some of the candidate structures of low energy.

### A. Total energy consideration

We have studied the total energy before by the LDA calculation for the  $\beta$ -tin and the Cs-IV structures<sup>22</sup> in the atomic phase and compared those with earlier calculations.<sup>21</sup> The GGA changes the optimum bond length and the total energy, so it may change the stable region of each structure. In order to check this, we recalculated the total energies in the GGA for some of the low-energy structures. In the calculation, we optimized the bond length at each density for fixed molecular orientation of  $(\theta, \phi) = (55^\circ, 43.5^\circ)$  in the  $Pca2_1$  and optimized the bond length for  $\theta = 60^\circ$  in the  $Cmca$ . The  $\beta$ -tin and Cs-IV structures in the atomic phase are optimized at each density.

The total energy in the GGA decreases somewhat from that in the LDA for both molecular and atomic phases. The decreases are larger for the structures in the molecular phase than those for the atomic phase. The results of the GGA increase the pressure of the equation of state by about 7–8 %

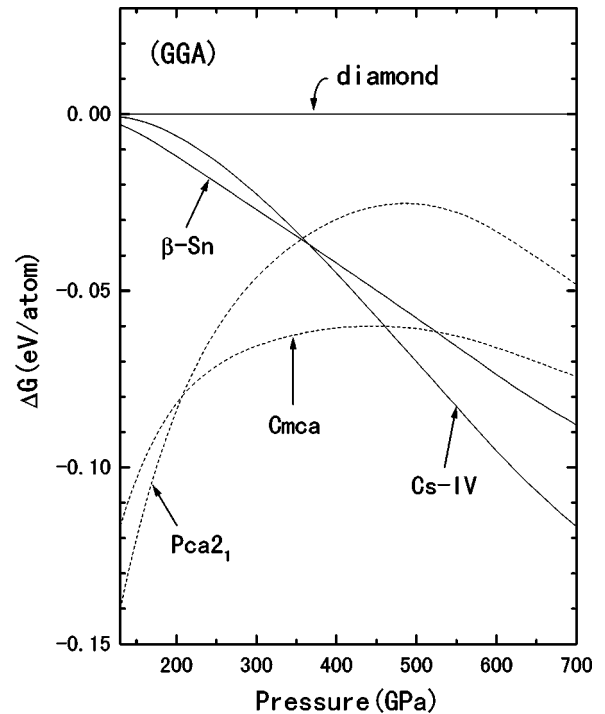


FIG. 10. Gibbs free-energy differences  $\Delta G = G - G_{\text{diamond}}$  per atom, calculated from the total energies in the GGA. The solid lines represent the curves for the atomic phase and the broken lines for the molecular phase. The diamond structure is taken to be the reference.

at megabar pressures in the molecular phase. The increase is much less in the atomic phase. The free energy difference among structures are compared in Fig. 10.

In the GGA, the free energy curve of the  $Pca2_1$  crosses with that of  $\beta$  tin or Cs-IV at  $\sim 350$  GPa, while, in the LDA, the curve of the  $Pca2_1$  crosses with that of  $\beta$  tin at around  $\sim 260$  GPa.<sup>22</sup> The recently calculated  $Cmca$  structure is lowest at pressures from 200 to 450 GPa, which widens the pressure range of the stable molecular phase to  $\sim 450$  GPa. We note that the  $Cmca$  structure has the closed band gaps above  $\sim 50$  GPa in the GGA.

Our results of the total energy calculation show that the  $Cmca$  structure has lower energy than the  $Pca2_1$  at densities higher than  $r_s = 1.40$  ( $P \sim 200$  GPa) though the results need further optimization with respect to the orientations of the molecules for both structures. The  $Cmc2_1$  structure with molecular centers displaced from the hcp sites has nearly same energy as that of the  $Cmca$  structure at  $r_s = 1.40$ , which is shown in Fig. 9. We note that the  $Cmc2_1$  also may need optimization with respect to the molecular orientations.

We have not included the zero-point energy of the proton motions in the total energy which is reported to be nearly the same for the structures with same lattice of the molecular centers.<sup>26</sup> The zero-point energy may change the transition pressures from a structure in the molecular phase to another structure with different lattice of the molecular centers or to the monoatomic phase, which remains for future studies.<sup>25,26</sup>

### B. Possible structures in the molecular phase at megabar pressures

Let us study the possible structures at megabar pressures from the vibrational modes and their frequencies and the total energies.

Our calculations are performed for structures in which the molecules are oriented in some patterns and we may not be able to compare the results with the experimental ones in the phases where the molecules are in the rotating state or in the states of large orientational fluctuations. However, we compared the results with experiments there, in the previous sections for some modes. We think that our treatment can approximately deal with the frequencies of the vibrons and the midlying phonons, which would not couple significantly with the librions owing to the large difference of the frequencies.

The calculated frequencies of the out-of-phase vibronic modes are higher than the in-phase mode, for all structures studied. The frequencies of the midlying phonon modes in the structures with hcp molecular centers and in the  $Pa3$  structure are in good agreement with the experiments, while that in the  $Cmca$  structure, in which the molecules are not on the hcp lattice sites, is a little deviated. Those results are common in both the GGA and the LDA.

The calculated vibron frequencies and their pressure dependences of the  $Cmc2_1$  structure with molecules on the hcp sites seem to be in good agreement with the experiments, where both vibrons are IR active as well as Raman. If more than two symmetry allowed Raman or IR vibron lines are really observed, the  $Cmc2_1$  structure is ruled out. We note that recent experiments have reported possibility of more vibron lines<sup>11,16,50</sup>. The number of low-lying modes in this structure is also smaller than that reported by the experiment.<sup>16</sup>

The vibron frequencies for the  $Pca2_1$  are in good agreement with the experiments in phase II. The anharmonicity may somewhat reduce the frequency in phase III, as was discussed in the previous section. In this structure, four Raman active vibronic modes (one is in-phase and the other three are out-of-phase) and three IR active vibronic modes (one is in-phase and the other two are out-of-phase) are expected as is shown in Table I with their frequencies in Fig. 3, and more lines of low-lying modes than in the  $Cmc2_1$  are also expected. The total energy of the  $Pca2_1$  structure is lowest of all hcp structures studied so far at pressures lower than  $\sim 200$  GPa.

In the  $Pa3$  structures the calculated vibron frequencies do not soften at high pressures, especially in phase III, which is similar to those of the  $Pca2_1$ , as is shown in Fig. 6. For this structure we calculated the frequencies only in the LDA, so the vibron frequencies in the GGA will become higher than those studied here. The band gaps in the LDA persist over 200 GPa in the  $Pa3$ . As for the phononlike modes, the frequency of the  $T_u$  mode is very close to the experiment.

The  $Pa3$  structure, in which the molecules sit on the fcc sites, has no IR active vibron, which contradicts the experimental results. Goncharov *et al.* proposed possibility of this structure in phase II in view of the point that they could not observe the Raman phonon there.<sup>16</sup> Our results of the frequencies may not exclude the possibility of the  $Pa3$  structure in phase II, if the weak IR activity of the vibrons comes from strains.<sup>16</sup> The frequency of the midlying phonon mode in the  $Pa3$ , which is IR active, is in good agreement with the experiment in phase III but the  $Pa3$  structure will be excluded in phase III because strong IR vibron is observed in the experiments, which suggests that the IR activity of the

vibron is symmetry allowed. We note that the LDA energy of this structure is higher than those of the hcp structures.<sup>18,22</sup>

The vibron frequencies of the  $m$ -hcp and the  $Cmca$ , in which the band gaps are closed at low densities, are considerably lower than the experiments. The frequency of the phonon mode in the  $Cmca$  structure is higher than that in the structures with hcp lattice of the molecular centers and is much higher than the experiments. The  $Cmca$  structure will be excluded at pressures lower than  $\sim 200$  GPa. However the total energy of the  $Cmca$  becomes lower than that of the  $Pca2_1$  structure at pressures higher than  $\sim 200$  GPa and may become lower than the  $Cmc2_1$  at further high densities, even if the full optimization of the displacement of the molecular centers and the molecular orientations are done in the  $Cmc2_1$ .

Last, we mention the low-lying librational modes. The behavior of the pressure dependences of the calculated frequencies for low-lying librational modes is somewhat different than those of the experiments as can be seen by the comparison of the results of the  $Cmc2_1$  given in Fig. 3 with the experiments.<sup>13,16</sup> Our frequencies for those modes decrease slowly as the pressure is decreased, while the experimental values of the frequencies decrease rapidly from the values in phase III and almost vanish at  $\sim 70$  GPa if the curves are extrapolated into phase II.<sup>13</sup> This behavior may be thought to be related with the large orientational fluctuation of the molecules, which cannot be treated by the present harmonic approximation, if the orientational order-disorder transition occurs at the II-III phase boundary. The quantum fluctuation of the molecular orientation will be important even after the orientational order occurred.

## VI. CONCLUSION AND REMARKS

The GGA for the exchange-correlation energy improves the results of the LDA for the compressed hydrogen on two points. One is that it widens the band gap through the shorter bond length and through the effect of widening band gaps inherent to the GGA in the molecular phase and the other is that it improves the vibron frequencies though the mid-lying phonon modes are not affected by the GGA.

Our calculation shows that the band gap closures affect the vibron frequencies considerably at megabar pressures. The band gap closure is sensitive to the bond length. The frequencies of the phononlike modes are rather insensitive to the molecular orientations.

According to our calculation in the harmonic approximation the most probable structure in phase III is  $Cmc2_1$ , although we cannot rule out the  $Pca2_1$  because the anharmonic terms may work to shift the vibron frequency towards the experimental values. The  $Pca2_1$  is most probable in phase II, if the molecules are in the orientational order in phase II. The total energies of the  $Pca2_1$  and the  $Cmc2_1$  are close with each other at megabar pressures.

Although vibrational frequencies for the  $Pa3$ , another candidate structure, is compatible with the experimental results in phase II, this structure has a total energy higher than the hcp structures in the pressure range of phase II,<sup>18,21,22</sup> and has no IR active vibron modes in the pure systems. However, a weak IR signal may be observed in the mixed system of the ortho- and para-species<sup>12</sup> or in the strained system, where the

present analysis of the activities cannot be applied. If the  $Pa3$  structure is realized in phase II, the midlying phonon mode can be observed in the IR experiments.<sup>8</sup>

Studies of the quantum fluctuation of the molecular orientation will be needed to know the behaviors of the low-lying librational modes. Our results show that the mixing of the librational motions with the phonon ones is large. So in such studies the coupling of the librational motion with the motions of the molecular centers<sup>45</sup> should be taken into account instead of studying the systems in which the molecular centers are fixed at the lattice points and considering only the orientational motions.<sup>51,52</sup>

Our present results suggest that the metalization occurs at pressure higher than  $\sim 200$  GPa but lower than  $\sim 450$  GPa by the transformation from a structure with open band gap to a structure with closed band gaps in the molecular phase, for example, transformation from the  $Cmc2_1$  to the  $Cmca$ , or

by the band overlapping in the same structure, for example, in the  $Cmc2_1$  with the displacement of the molecular centers. The pressure at which the transformation occurs depends upon the structure in the molecular phase as well as that in the atomic phase and needs more study with full optimization of the molecular orientations and the bond lengths simultaneously. The estimation of the band gap may also be needed by the calculation beyond the GGA.<sup>20</sup>

## ACKNOWLEDGMENTS

The authors wish to acknowledge discussions with H. Miyagi. This work was supported in part by a Grant-in-Aid for the Scientific Research of the Japanese Ministry of Education (No. 08304026) and the CREST JST. The computations were done at the Institute of Laser Engineering, Osaka University.

\*Present address: Japan Synchrotron Radiation Research Institute, Mikazuki, Sayo, Hyogo 679-5198, Japan.

<sup>1</sup>E. Wigner and H. B. Huntington, *J. Chem. Phys.* **3**, 764 (1935).

<sup>2</sup>H. K. Mao and R. J. Hemley, *Rev. Mod. Phys.* **66**, 671 (1994), and references therein.

<sup>3</sup>S. T. Weir, A. C. Mitchell, and W. J. Nellis, *Phys. Rev. Lett.* **76**, 1860 (1996), and references therein for earlier dynamic compression experiments.

<sup>4</sup>See the latest paper, for example, C. F. Richardson and N. W. Ashcroft, *Phys. Rev. Lett.* **78**, 118 (1997).

<sup>5</sup>T. W. Barbee III and M. L. Cohen, *Phys. Rev. B* **43**, 5269 (1991).

<sup>6</sup>M. Hanfland, R. J. Hemley, and H. K. Mao, *Phys. Rev. B* **43**, 8767 (1991); J. H. Eggert, F. Moshary, W. J. Evans, H. E. Lorenzana, K. A. Goettel, I. F. Silvera, and W. C. Moss, *Phys. Rev. Lett.* **66**, 193 (1991); A. L. Ruoff and C. A. Vanderborgh, *ibid.* **66**, 754 (1991); **71**, 4279(E) (1993).

<sup>7</sup>L. B. Da Silva, P. Celliers, G. W. Collins, K. S. Budil, N. C. Holmes, T. W. Barbee, Jr., B. A. Hammel, J. D. Kilkenny, R. J. Wallace, M. Ross, R. Cauble, A. Ng, and G. Chiu, *Phys. Rev. Lett.* **78**, 483 (1997).

<sup>8</sup>N. H. Chen, E. Sterer, and I. F. Silvera, *Phys. Rev. Lett.* **76**, 1663 (1996).

<sup>9</sup>R. J. Hemley, H. K. Mao, A. F. Goncharov, M. Hanfland, and V. Struzhkin, *Phys. Rev. Lett.* **76**, 1667 (1996).

<sup>10</sup>P. Loubeyre, R. LeToullec, D. Hausermann, M. Hanfland, R. J. Hemley, H. K. Mao, and L. W. Finger, *Nature (London)* **383**, 702 (1996).

<sup>11</sup>L. Cui, N. H. Chen, S. J. Jeon, and I. F. Silvera, *Phys. Rev. Lett.* **72**, 3048 (1994).

<sup>12</sup>L. Cui, N. H. Chen, and I. F. Silvera, *Phys. Rev. B* **51**, 14 987 (1995); **57**, 656(E) (1998), and references therein.

<sup>13</sup>I. I. Mazin, R. J. Hemley, A. F. Goncharov, M. Hanfland, and H. K. Mao, *Phys. Rev. Lett.* **78**, 1066 (1997).

<sup>14</sup>A. F. Goncharov, I. I. Mazin, J. H. Eggert, R. J. Hemley, and H. K. Mao, *Phys. Rev. Lett.* **75**, 2514 (1995).

<sup>15</sup>A. F. Goncharov, J. H. Eggert, I. I. Mazin, R. J. Hemley, and H. K. Mao, *Phys. Rev. B* **54**, R15 590 (1996).

<sup>16</sup>A. F. Goncharov, R. J. Hemley, H. K. Moe, and J. Shu, *Phys. Rev. Lett.* **80**, 101 (1998).

<sup>17</sup>For the hydrogen (deuterium) molecule para designates the even (odd) rotational quantum number  $J$  and ortho the odd (even)  $J$  species.

<sup>18</sup>T. W. Barbee III, A. Garcia, M. L. Cohen, and J. L. Martins, *Phys. Rev. Lett.* **62**, 1150 (1989).

<sup>19</sup>N. W. Ashcroft, *Phys. Rev. B* **41**, 10 963 (1990), and references therein.

<sup>20</sup>H. Chacham and S. G. Louie, *Phys. Rev. Lett.* **66**, 64 (1991).

<sup>21</sup>H. Nagara and T. Nakamura, *Phys. Rev. Lett.* **68**, 2468 (1992).

<sup>22</sup>K. Nagao, H. Nagara, and S. Matsubara, *Phys. Rev. B* **56**, 2295 (1997).

<sup>23</sup>D. M. Straus and N. W. Ashcroft, *Phys. Rev. Lett.* **38**, 415 (1977).

<sup>24</sup>M. P. Surh, T. W. Barbee III, and C. Mailhot, *Phys. Rev. Lett.* **70**, 4090 (1993).

<sup>25</sup>V. Natoli, R. M. Martin, and D. M. Ceperley, *Phys. Rev. Lett.* **70**, 1952 (1993).

<sup>26</sup>V. Natoli, R. M. Martin, and D. M. Ceperley, *Phys. Rev. Lett.* **74**, 1601 (1995).

<sup>27</sup>J. Kohanoff, S. Scandolo, G. L. Chiarotti, and E. Tosatti, *Phys. Rev. Lett.* **78**, 2783 (1997).

<sup>28</sup>J. S. Tse and D. D. Klug, *Nature (London)* **378**, 595 (1995).

<sup>29</sup>J. H. Eggert, H. K. Mao, and R. J. Hemley, *Phys. Rev. Lett.* **70**, 2301 (1993); M. I. M. Scheerboom and J. A. Schouten, *Phys. Rev. B* **53**, R14 705 (1996).

<sup>30</sup>K. Nagao and H. Nagara, *Phys. Rev. Lett.* **80**, 548 (1998). The word "megabar" (Mbar) has been misprinted in the paper as "mbar."

<sup>31</sup>See, for example, J. C. Slater, *J. Chem. Phys.* **57**, 2389 (1972).

<sup>32</sup>U. von Barth and L. Hedin, *J. Phys. C* **5**, 1629 (1972). Another choice of the exchange-correlation potential, for example, by Ceperley and Alder [D. M. Ceperley and B. J. Alder, *Phys. Rev. Lett.* **45**, 566 (1980); J. P. Perdew and A. Zunger, *Phys. Rev. B* **23**, 5048 (1981)] gives no significant differences of the results.

<sup>33</sup>See, for example, B. Edwards, N. W. Ashcroft, and T. Lenosky, *Europhys. Lett.* **34**, 519 (1996), and references therein.

<sup>34</sup>See standard texts of the group theory, for example, M. Lax, *Symmetry Principles in Solid State and Molecular Physics* (Wiley-Interscience, New York, 1974).

<sup>35</sup>H. Nagara (unpublished). The same method was used in Refs. 21, 22 and 30.

<sup>36</sup>See, for example, J. P. Perdew, J. P. Chevary, S. H. Vosko, K. A. Jackson, M. R. Pederson, D. J. Singh, and C. Fiolhais, *Phys. Rev. B* **46**, 6671 (1992); **48**, 4978(E) (1993), and references therein.

- <sup>37</sup>J. P. Perdew, K. Burke, and M. Ernzerhof, *Phys. Rev. Lett.* **80**, 891 (1998); Y. Zhang and W. Yang, *ibid.* **80**, 890 (1998).
- <sup>38</sup>J. P. Perdew, K. Burke, and M. Ernzerhof, *Phys. Rev. Lett.* **77**, 3865 (1996); **78**, 1396(E) (1997).
- <sup>39</sup>R. J. Hemley, H. K. Mao, and J. F. Shu, *Phys. Rev. Lett.* **65**, 2670 (1990).
- <sup>40</sup>B. Edwards and N. W. Ashcroft, *Nature (London)* **388**, 652 (1997).
- <sup>41</sup>E. Kaxiras, J. Broughton, and R. J. Hemley, *Phys. Rev. Lett.* **67**, 1138 (1991).
- <sup>42</sup>I. I. Mazin and R. E. Cohen, *Phys. Rev. B* **52**, R8597 (1995).
- <sup>43</sup>J. Kohanoff, *Proceedings of the Adriatico Research Conference: Simple Systems at High Pressures and Temperatures: Theory and Experiment*, ICTP Science Abstract No. 23, URL [http://www.ictp.trieste.it/pub\\_off/sci-abs/smr999](http://www.ictp.trieste.it/pub_off/sci-abs/smr999) (ICTP, Trieste, October, 1997).
- <sup>44</sup>A. Alavi, *Proceedings of the Adriatico Research Conference: Simple Systems at High Pressures and Temperatures: Theory and Experiment*, ICTP Science Abstract No. 18, URL [http://www.ictp.trieste.it/pub\\_off/sci-abs/smr999](http://www.ictp.trieste.it/pub_off/sci-abs/smr999) (ICTP, Trieste, October, 1997).
- <sup>45</sup>T. Cui, E. Cheng, B. J. Alder, and K. B. Whaley, *Phys. Rev. B* **55**, 12 253 (1997).
- <sup>46</sup>H. M. James, *Phys. Rev.* **167**, 862 (1968); H. Miyagi and T. Nakamura, *Prog. Theor. Phys.* **37**, 641 (1967); A. I. Kitaigorodskii and K. V. Mirskaya, *Sov. Phys. Crystallogr.* **10**, 121 (1965).
- <sup>47</sup>R. A. Cowley, *Adv. Phys.* **12**, 421 (1963).
- <sup>48</sup>R. J. Hemley, H. K. Mao, and M. Hanfland, in *Molecular Systems under High Pressure*, edited by R. Pucci and G. Piccino (Elsevier, Amsterdam, 1991), p. 223.
- <sup>49</sup>I. J. Robertson and M. C. Payne, *J. Phys. C* **2**, 9837 (1990).
- <sup>50</sup>M. Hanfland, R. J. Hemley, and H. K. Mao, *Phys. Rev. Lett.* **70**, 3760 (1993).
- <sup>51</sup>K. J. Runge, M. P. Surh, C. Mailhiet, and E. L. Pollock, *Phys. Rev. Lett.* **69**, 3527 (1992).
- <sup>52</sup>E. Kaxiras and Z. Guo, *Phys. Rev. B* **49**, 11 822 (1994).
- <sup>53</sup>M. Hanfland, R. J. Hemley, H. K. Mao, and G. P. Williams, *Phys. Rev. Lett.* **69**, 1129 (1992).
- <sup>54</sup>H. E. Lorenzana, I. F. Silvera, and K. A. Goettel, *Phys. Rev. Lett.* **64**, 1939 (1990).